Title
Degradation in intrinsic connectivity networks across the Alzheimer's disease spectrum

Journal
Alzheimer's & Dementia Diagnosis Assessment & Disease Monitoring, 5(1)

ISSN
2352-8729

Authors
Nuttall, Rachel
Pasquini, Lorenzo
Scherr, Martin
et al.

Publication Date
2016

DOI
10.1016/j.dadm.2016.11.006

Peer reviewed

Alzheimer's & Dementia: Diagnosis, Assessment & Disease Monitoring 5 (2016) 35-42

Neuroimaging

Degradation in intrinsic connectivity networks across the Alzheimer's disease spectrum

Rachel Nuttall[a,b,*], Lorenzo Pasquini[b,c], Martin Scherr[b,d,e], Christian Sorg[b,c,d], for the Alzheimer's Disease Neuroimaging Initiative[1]

[a]Department of Psychology, Ludwig Maximilian University Munich, Munich, Germany
[b]TUM-Neuroimaging Center, Neuro-Kopf-Zentrum, Technische Universität München, Munich, Germany
[c]Department of Neuroradiology, Technische Universität München, Munich, Germany
[d]Department of Psychiatry, Technische Universität München, Munich, Germany
[e]Doppler Klinik, Division of Neuroradiology, Paracelsus Medical University Salzburg, Salzburg, Austria

Abstract

Introduction: Changes in intrinsic functional connectivity (iFC) have been reported at various stages of the Alzheimer's disease (AD) spectrum. We aimed to investigate such alterations over a variety of large-scale intrinsic brain networks (iBNs) across the spectrum of amyloid β positivity and uncover their relation to cognitive impairment.

Methods: Eight iBNs were defined from resting-state functional magnetic resonance imaging data. In amyloid β–positive healthy subjects, prodromal, and AD patients (N = 70), within-network iFC (intra-iFC) and between-network iFC (inter-iFC) were correlated with scores of cognitive impairment.

Results: Across all iBNs, a general degradation in intra-iFC along the scale of cognitive impairment severity was found. Only subtle changes in inter-iFC were identified.

Discussion: Across the AD spectrum, changes in iFC that are strongly related to cognitive impairment occur within an extensive variety of networks.

Keywords: Alzheimer's disease; Intrinsic brain networks; Intrinsic functional connectivity; Resting-state fMRI; Cognitive impairment

1. Introduction

Alzheimer's disease (AD) is the major cause of age-related dementia with 46.8 million people worldwide estimated to be living with dementia [1]. AD is a neurodegenerative disorder characterized by progressive amyloid β (Aβ) pathology, tau-related pathology, and cell loss [2]. In particular, Aβ pathology is characterized by progressive Aβ plaque accumulation, starting in the isocortex several years before first cognitive symptoms arise, and interacting in a complex way with both brain activity and rising tau-related pathology [3]. In the context of manifest Aβ plaques, changes in cortical activity occur, particularly in relation to slowly fluctuating ongoing (i.e., intrinsic) activity and intrinsic functional connectivity (iFC) [4–10]. Changes in

Institution of origin: Klinikum rechts der Isar, Technische Universität München, Ismaninger Strasse 22, 81675 Munich, Germany.

Disclosure: The authors declare no competing financial interests.

[1]Data used in the preparation of this article were obtained from the Alzheimer's Disease Neuroimaging Initiative (ADNI) database (adni.loni.ucla.edu). As such, the investigators within the ADNI contributed to the design and implementation of ADNI and/or provided data but did not participate in analysis or writing of this report. A complete listing of ADNI investigations can be found at http://adni.loni.ucla.edu/wp-content/uploads/how_to_apply/ADNI_Acknowledgement_List.pdf.

*Corresponding author. Tel.: +49-89-4140-7666; Fax: +49-89-4140-4887.

E-mail address: rachelnutt3012@hotmail.com

http://dx.doi.org/10.1016/j.dadm.2016.11.006

iFC are detectable in vivo by changes in correlated blood oxygenation level dependent (BOLD) fluctuations as measured by resting-state functional magnetic resonance imaging (rsfMRI).

In more detail, slow (<0.1 Hz) ongoing fluctuations of activity occur in the absence of a task and findings of coherence between these fluctuations across spatially distributed brain regions have led to the proposition of resting-state or so-called intrinsic brain networks (iBNs). A wide variety of primary sensory and motor, default mode, and "attentional" iBNs have been identified, which show high reproducibility [11,12]. One such iBN is the default mode network (DMN), consisting of discrete regions of the bilateral parietal, prefrontal, and temporal cortices that show coherent hemodynamic fluctuations at rest [13].

Alterations in iFC within (intra-iFC) and between (inter-iFC) iBNs have been reported at various stages across the AD spectrum. With increasing mild cognitive impairment (MCI) and dementia, both increases and decreases in intra-iFC have been reported in AD [14–16], alongside decreases in inter-iFC [14,16]. In terms of specific iBNs, iFC changes within the DMN in AD have been extensively studied, showing disruptions both preclinically in Aβ-positive healthy control subjects [6,17] and as a function of cognitive impairment [18].

However, the pattern of alterations in iFC within and between an extensive variety of iBNs across the whole AD spectrum of Aβ positivity remains unknown.

Consequently, the present study focused on three main questions: (1) How do changes in iFC within iBNs (i.e., intra-iFC) relate to cognitive impairment across the whole AD spectrum? (2) How do changes in iFC between iBNs (i.e., inter-iFC) relate to cognitive impairment across the whole AD spectrum? (3) How do these intra-iFC and inter-iFC changes relate to one another?

To test these questions, a sample (N = 161) of multimodal imaging and neuropsychological data sets from Aβ-negative, Aβ-positive preclinical, prodromal, and clinically manifest AD subjects were analyzed. Statistical analyses were restricted to Aβ-positive subjects only to restrict the analysis to subjects on an AD-related trajectory of cognitive impairment. A spatial independent component analysis (ICA) was used to estimate iFC across eight iBNs in rsfMRI data. Scores of intra-iFC and inter-iFC were correlated with scores on a continuous measure of AD-related cognitive impairment and with one another.

2. Methods

Data were retrieved from the Alzheimer's Disease Neuroimaging Initiative (ADNI) database (http://adni.loni.usc.edu). Launched in 2003, ADNI supports the investigation and development of treatments against the progression of AD via a $60 million 5-year partnership between various institutes and organizations. This longitudinal multisite study aims to combine various findings of clinical, genetic, imaging, and biospecimen biomarkers across the MCI and AD spectrum to work toward a cohesive understanding of AD and the development of efficacious treatment options against MCI and AD progression. For further information, see https://adni.loni.usc.edu/.

2.1. Participants

Subject data sets complete with rsfMRI, structural MRI, and F^{18}-AV-45-PET (positron emission tomography) scans were retrieved from the ADNI-GO and ADNI2 study phase databases of ADNI, reaping a starting sample size of 161 subjects. When more than one rsfMRI or structural MRI scan was available, those that were acquired within 3 months of one another and met quality control measures were chosen. Subjects whose scans were more than 3 months apart were excluded (n = 12). After visual inspection of the data, subjects were excluded because of imaging artifacts (n = 20), field-of-view cuts (n = 6), and excessive head motion parameters (n = 2) (for exact criteria see subsequently). Patients identified as Aβ negative (see Section 2.3.1 for identification criteria) were also excluded (n = 31). Thus, a high-quality sample of 90 subjects was further analyzed, representing a range of healthy control subjects and the whole spectrum of AD-related cognitive impairment: Aβ-negative healthy control subjects (HC−; n = 20), Aβ-positive healthy control subjects (HC+; n = 9), early MCI (eMCI+; n = 21) and late MCI (lMCI+; n = 18), and AD patients (AD+; n = 22). Healthy control subjects are in a preclinical stage in which there are no signs of depression, MCI, or dementia, with or without the presence of Aβ accumulation (HC+ and HC−, respectively) [19]. MCI patients present concerns of memory decline but do not surpass the threshold of functional impairment to be classified as demented and do not show impairments in other cognitive domains; hence, these subjects present amnestic MCI. The ADNI database subdivides amnestic MCI into two stages, namely eMCI and lMCI, differentiated on the basis of the severity of episodic memory impairment [20], assessed via the Logical Memory II subscale (Delayed Paragraph Recall, Paragraph A only from the Wechsler Memory Scale-Revised) [21]. Patients in the AD group meet the criteria for probable AD, as stated by the National Institute of Neurological and Communicative Disorders and Stroke and the Alzheimer's Disease and Related Disorders Association [22]. Further information on the respective inclusion criteria can be found at https://adni.loni.usc.edu/wp-content/adni2-procedures-manual.pdf.

All patients were Aβ positive, defined using a cutoff of 1.11 composite cortical standard uptake value ratio (SUVR) using the cerebellum as a reference [23] (for details see subsequently). Thus, all patients were following an AD-related dementia trajectory. See demographic information in Table 1. Further details on the ADNI guidelines in terms of clinical diagnosis and inclusion criteria can be found at http://adni.loni.usc.edu/methods/.

Table 1
Demographic and neuropsychological data

Variable	CN−	CN+	eMCI	lMCI	AD	*F* (*P* value)
N	20	9	21	18	22	
Mean age in years (SD)	74.6 (7.86)	76.26 (5.60)	71.22 (5.61)	73.56 (7.31)	73.32 (7.93)	1.01 (.407)
Sex (N female)	14	5	9	8	12	— (.445)
Mean ADAS Cog (Mod) score (SD)	9.55 (4.32)	9.22 (3.70)	14.14 (6.15)	20.5 (7.73)	35.55 (10.14)	44.5 (.000)

Abbreviations: AD, Alzheimer's disease; ADAS Cog, Alzheimer's Disease Assessment Scale-cognitive subscale; eMCI, early mild cognitive impairment; lMCI, late mild cognitive impairment; SD, standard deviation.

NOTE. Subjects in our sample included both healthy control subjects and patients covering the whole spectrum of AD-related cognitive impairment: Aβ-negative healthy control subjects (HC−), Aβ-positive healthy control subjects (HC+), eMCI+, lMCI+, and AD patients (AD+). Group comparisons: analysis of variance was conducted for all measures except sex (Kruskal-Wallis test).

2.2. Acquisition of cognitive impairment score

Scores on the Alzheimer's Disease Assessment Scale-cognitive subscale (ADAS Cog), reflecting cognitive impairment, were downloaded from the ADNI database. This measure evaluates the extent of cognitive impairment along a continuous scale, as a crucial symptom in the assessment of AD [24]. Consisting of 11 tests measuring memory, praxis, and language [25], a higher score indicates greater cognitive dysfunction, with a score of 5 or less relating to no cognitive impairment [26]. This instrument has been shown to be highly sensitive to detect changes in both mild and severe dementia [27], with high reliability and validity [28]. Scores of the modified version of the ADAS Cog (ADAS Cog (Mod)) were acquired; the original measure was modified to include two further items [29] that improved the sensitivity of the scale to cognitive changes in MCI patients [30]. See http://www.dementia-assessment.com.au/cognitive/ADAS_Packet.pdf for further details on the scale.

2.3. Acquisition and analysis of imaging data

Across multiple centers, several 3 T MRI scanners were used to acquire MRI data: T1-weighted sagittal 3D MPRAGE sequences for structural MRI and rsfMRI sequences on Philips systems. F^{18}-AV-45-PET scans were acquired according to scanner-specific protocols. To standardize scans, images underwent preprocessing correction steps. For further information on scan acquisition protocols and correction steps for standardization, please refer to http://adni.loni.usc.edu/data-samples/.

2.3.1. PET data preprocessing

For each subject, F^{18}-AV-45-PET images were rigidly coregistered with the individual's corresponding structural MRI image, skull-stripped, and normalized to the Montreal Neurological Institute (MNI) space using the normalization parameters acquired previously. Thus, structural MRI, fMRI, and PET images shared the same dimensions and space. The images were converted to composite cortical SUVRs by scaling voxel values to the whole cerebellar region. On the basis of these values, Aβ-negative patients were identified and excluded from further analysis, defined by an SUVR lower than 1.11 with the whole cerebellum as reference, according to ADNI guidelines of F^{18}-AV-45-PET analyses [23].

2.3.2. fMRI data preprocessing

Preprocessing was conducted using SPM12 (Wellcome Department of Cognitive Neurology, London) and the Data Processing Assistant for Resting-State fMRI toolbox (http://rfmri.org/DPARSF) [31]. After the first 10 functional images of every subject were removed, slice-timing correction for the removal of slice-dependent time shifts acquired during interleaved scanning was performed and rigid body correction for head movement through realignment to the mean fMRI image. No excessive head motion was identified (i.e., cumulative translation or rotation 3 mm or 3° and mean point-to-point translation or rotation 0.15 mm or 0.1°). Framewise displacement was not different across groups of Aβ-positive healthy control subjects, eMCI, lMCI, and AD patients ($P > .05$, ANOVA). The T1 structural images were coregistered to the mean fMRI image using rigid registration and segmented into gray matter (GM), white matter, and cerebrospinal fluid and registered to the MNI stereotactic space with unified segmentation. Nuisance waveform regression of white matter, cerebrospinal fluid, head motion, and the averaged whole-brain signal were performed, following which the functional MRI images were normalized into the MNI stereotactic space using the same normalization parameters acquired previously, with an isotropic $3 \times 3 \times 3$ mm^3 voxel size and smoothed with a $6 \times 6 \times 6$ mm^3 Gaussian kernel [32].

Furthermore, our analysis was replicated on "scrubbed" fMRI data, in which movement-induced artifacts had been censored by the identification and exclusion of volumes possibly contaminated by movement [33]. This was conducted by the calculation of the root mean square of the translational and rotational head movement parameters. Volumes that exceeded a predefined threshold of the root mean square of such parameters (0.25 mm + 2 standard deviations of all subjects) were excluded from further analyses [34].

2.3.3. iBN detection from rsfMRI data and analysis of relationship between iBNs and cognitive scores

iBNs were detected via group ICA from preprocessed rsfMRI data by a two-step procedure: first, independent

iBN templates were defined in Aβ-negative healthy control subjects via ICA, and then templates were used to analyze iBNs in Aβ-positive subjects. More specifically, the detrended images of HC− subjects were decomposed into spatially independent components reflecting iBNs via a group ICA [35], within the Group ICA of fMRI Toolbox (GIFT) (http://www.icatb.sourceforge.net). ICA extracts discrete temporally coherent patterns of activity between spatially distributed brain regions from the mixed rsfMRI signal [36]. Sixty-four components were estimated and analyzed using the Infomax algorithm and the Icasso software [37] with 40 runs to assess the reliability of the ICA algorithm. Multiple spatial regression analyses of the components were applied on network templates available online from a previous multicenter study [12]. The components were identified as iBNs based on inspection of the power spectrums and regression coefficient values, alongside visual judgment of anatomic accuracy. Eight components judged as reliably reflecting iBNs (i.e., showing strong anatomic accuracy, strong regression coefficients, and power) were chosen for further analysis (see Fig. 1). Then, for each subject, an individual independent component reflecting an iBN was derived via back-reconstruction as implemented in GIFT. The component was composed of the network's time course and spatial map of *z*-scores.

One-sample *t* tests on *z*-maps were conducted on all identified network components of HC− subjects, from which network templates were created. These templates were multiplied with an averaged GM mask created from the segmented GM images derived from the structural MRI data of Aβ-positive subjects only, binarized with a probability threshold of 0.4. This was conducted to restrict the network templates to the GM regions present in the Aβ-positive subjects. ICA of preprocessed fMRI data of Aβ-positive subjects was performed in the same way as for Aβ-negative subjects, resulting in spatial *z*-maps and corresponding time

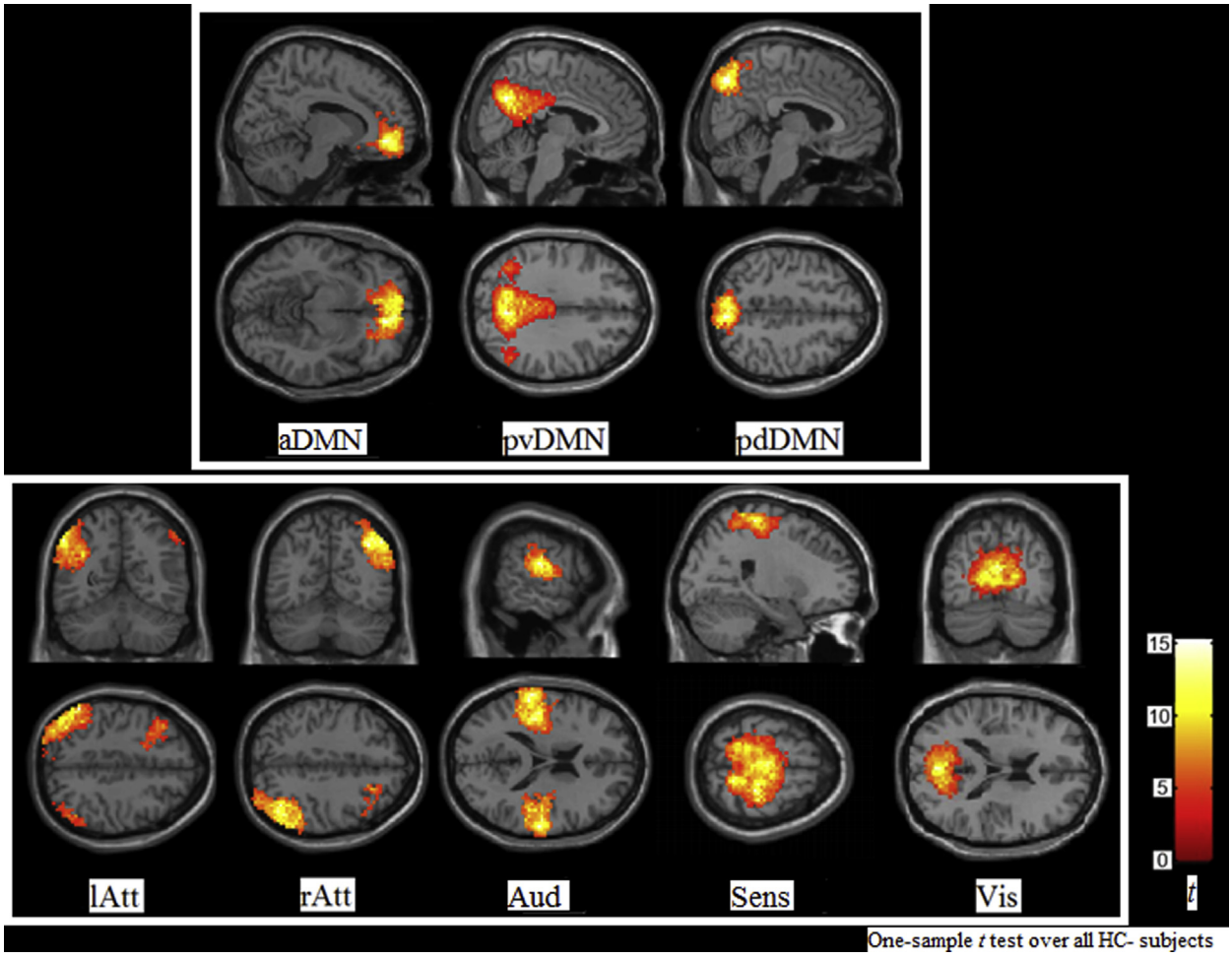

Fig. 1. Chosen intrinsic brain networks (iBNs). Across a data sample of cognitively normal amyloid β–negative healthy control subjects, eight independent components of fMRI data were identified as iBNs using previously defined templates [12], shown as statistical parametric maps (one-sample *t* test $P < .001$, uncorrected, height threshold $t = 3.58$, extent threshold $k = 100$), overlaid on a high-resolution canonical T1 image from the MNI series. For each iBN, two columnized images are shown. The top row shows the three default mode subnetworks: anterior (aDMN), posterior-ventral (pvDMN), and the posterior-dorsal (pdDMN). The bottom row displays the left attention (lAtt), the right attention (rAtt), the auditory (Aud), the sensorimotor (Sens), and the visual (Vis) iBNs. The color bar from red to yellow-white represents *t* values, ranging from 3.58 to 15. Abbreviations: fMRI, functional magnetic resonance imaging; MNI, Montreal Neurological Institute.

courses for each iBN and subject, respectively. One-sample *t* tests on *z*-maps were then conducted on the identified iBNs in all Aβ-positive subjects, on which the network templates were overlaid to extract mean *z*-scores of intra-iFC for each iBN. Hence, scores of intra-iFC reflect the value of statistically significant standardized coherence in BOLD signal time series between any two voxels in the network, averaged across all possible voxel pairs within the network template. These scores were then inputted into the Statistical Package for the Social Sciences (SPSS) software, version 22.0 (IBM corporation, Armonk, NY, USA) [38] for a partial correlation coefficient (*r*) analysis, controlling for age, sex, and GM atrophy, with scores of cognitive impairment (Pearson's, $P < .05$, Bonferroni corrected for multiple comparisons).

Concerning inter-iFC between iBNs, mean network time courses of pairs of networks, as calculated within the Resting-State fMRI Data Analysis Toolkit (REST) [39] were correlated via Pearson's correlation, respectively. Pearson's (*r*) maps were transformed into *z*-maps using the Fisher's *z*-transform. Hence, scores of inter-iFC reflected the standardized value of correlation between the average BOLD time series of any two networks. These inter-iFC scores were then inputted into SPSS for a partial correlation analysis, controlling for age, sex, and GM atrophy, with scores of cognitive impairment (Pearson's, $P < .05$, Bonferroni corrected for multiple comparisons).

Inter-iFC scores were also analyzed for partial correlative relationships with intra-iFC *z*-scores controlling for age, sex, and GM atrophy in an exploratory approach seeking to understand whether changes in intra-iFC are related to changes in inter-iFC along the AD dementia spectrum.

3. Results

3.1. Intrinsic functional connectivity and cognitive impairment

3.1.1. Intra-iFC

Results showed a significant decline in iFC within all networks as cognitive impairment increased (see Table 2, Fig. 2). After a Bonferroni correction for multiple comparisons (corrected $a \leq 0.006$), this decline in iFC as a function of cognitive impairment severity was no longer significant within the right attention and sensorimotor networks.

3.1.2. Inter-iFC

The relationships between mean inter-iFC *z*-scores and cognitive impairment scores were investigated. After Bonferroni correction for multiple comparisons, no network pairs showed a significant correlation between inter-iFC and cognitive impairment (see Table 3). Results showed subtle trends toward a significant relationship between inter-iFC and cognitive impairment for the pair of posterior-ventral and posterior-dorsal DMNs (pvDMN-pdDMN; $P = .056$) and for the pdDMN and visual network pair (pdDMN-Vis; $P = .043$), but these trends did not survive Bonferroni correction for multiple comparisons (corrected $a \leq 0.006$).

Table 2
Correlations between intra-iFC scores and ADAS Cog (Mod) scores

	Correlation coefficient (*r*) (*P* value)	Linear regression
Intrinsic brain network	Control subjects: sex, age, GM atrophy	Adjusted R^2 (*P* value)
lAtt	**−0.386 (.001)***	0.131 (.001)
rAtt	−0.284 (.020)*	0.067 (.018)
aDMN	**−0.369 (.002)***	0.123 (.002)
pvDMN	**−0.566 (<.001)***	0.316 (<.001)
pdDMN	**−0.412 (.001)***	0.171 (<.001)
Aud	**−0.425 (<.001)***	0.170 (<.001)
Vis	**−0.381 (.001)***	0.135 (.001)
Sens	−0.263 (.032)*	0.057 (.026)

Abbreviations: ADAS Cog (Mod), modified version of the Alzheimer's Disease Assessment Scale-cognitive subscale; Aud, auditory network; iFC, intrinsic functional connectivity; lAtt, left attention network; pdDMN, posterior-dorsal default mode network; pvDMN, posterior-ventral default mode network; rAtt, right attention network; Sens, sensorimotor network; Vis, visual network.

NOTE. Pearson product-moment correlation coefficients (*r*), controlled for age, sex, and GM atrophy, which were significant after multiple comparison correction (corrected $a \leq .006$) are indicated by bold values. A linear regression was conducted and estimated adjusted R^2 values and associated analysis of variance model significance values are shown (see Fig. 2).

*Significant correlations at $P \leq .05$, before correction for multiple comparisons.

3.2. Intra-iFC and inter-iFC

No significant correlative relationships between iFC scores within and between networks were found (for all networks, $P > .1$).

4. Discussion

We investigated how alterations in iFC within and between an extensive variety of iBNs across the whole AD spectrum of Aβ positivity relate to cognitive impairment. Eight iBNs were defined from a spatial ICA and *z*-scores of mean intra-iFC and inter-iFC were correlated with scores of cognitive impairment. With increased cognitive impairment, we found a general decline in iFC within all iBNs. Only rather subtle decrements in iFC between certain iBNs were found to be associated with increased cognitive impairment, namely for the posterior DMN and visual network. Scores of iFC within and between iBNs were unrelated to one another. This study is the first to identify changes in iFC both within and between a large variety of iBNs in Aβ-positive subjects only, as a function of cognitive impairment. Findings suggest that AD is a disorder in which multiple brain networks are affected in an almost parallel mode, with the most substantial changes occurring in the functional connections within the networks themselves.

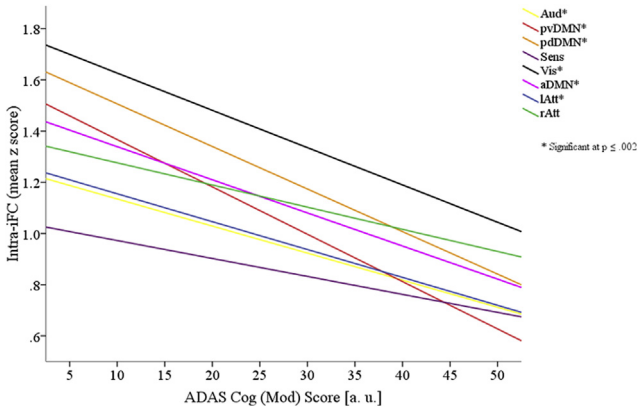

Fig. 2. Correlations of intra-iFC with cognitive impairment. Scatterplot with best-fitted lines shows iFC within each iBN (intra-iFC) as a function of ADAS Cog (Mod) score of cognitive impairment, arbitrary unit (a.u.). The following iBNs are displayed: auditory (Aud), posterior-ventral default mode network (pvDMN), posterior-dorsal default mode network (pdDMN), anterior default mode network (aDMN), sensorimotor (Sens), visual (Vis), left attention (lAtt), and right attention (rAtt). Greater z-scores indicate greater intrinsic functional coherence and larger ADAS Cog (Mod) scores indicate greater cognitive impairment. All partial Pearson product-moment correlation coefficients, controlled for age, sex, and GM atrophy, were significant at the $P < .05$ level; however, after correction for multiple comparisons ($a \leq .006$), the Sens and rAtt iBNs were no longer significant. Asterisks in the legend indicate those correlative curves that remained significant after multiple comparison correction. See Table 2 for corresponding correlation coefficients and significance values. Abbreviations: ADAS Cog (Mod), modified version of the Alzheimer's Disease Assessment Scale-cognitive subscale; iBN, intrinsic brain network; iFC, intrinsic functional connectivity.

4.1. Reduced iFC with increased cognitive impairment

4.1.1. Reductions in intra-iFC

With increased cognitive impairment, all eight iBNs showed reductions in intra-iFC (see Table 2 and Fig. 2). For all networks except the right attention and sensorimotor networks, these negative correlations between intra-iFC and cognitive impairment were robust, having survived correction for multiple comparisons and control over the potential covariates of age, sex, and GM atrophy.

4.1.2. Subtle reductions in inter-iFC

With increased cognitive impairment, iFC between certain networks was subtly reduced. These subtle changes were observed between the posterior DMNs and the visual network. However, as these findings did not survive correction for multiple comparisons, these findings must be interpreted with caution. Despite this, they do support previous findings of reductions in inter-iFC between specific networks as a function of cognitive impairment [14,16] and may indicate slight changes that occur in the connectivity between networks in AD, alongside the aforementioned intra-iFC changes.

These subtle decrements in inter-iFC were not significantly related to intra-iFC, suggesting that they may be markers of other reactive processes that occur in the brain with AD progression. Previous theoretical models have proposed a dynamic functional model of the resting brain that constantly fluctuates between various competitive states of iFC to achieve a resting state primed for optimal behavioral performance [40]. This leads to postulate that the subtle reductions in inter-iFC may be markers of the dynamic brain fluctuating through various states of iFC in an attempt to keep the resting brain in the most optimal state possible, given the challenges that the AD-affected brain faces, such as pathologic iFC patterns within iBNs.

4.2. Alzheimer's disease: A multiple network disorder

As a network involved in declarative memory processing [41], the DMN has long been the focus of research into disrupted iFC in AD. However, it is clear from our results and indeed the results of previous studies that AD can be

Table 3
Correlations between inter-iFC and ADAS Cog (Mod) scores

Correlation coefficient r (P value)
Control subjects: sex, age, GM atrophy

Network Pair	lAtt-	rAtt-	aDMN-	pvDMN-	pdDMN-	Vis-	Aud-	Sens-
lAtt								
rAtt	0.087 (.487)							
aDMN	0.039 (.757)	0.029 (.817)						
pvDMN	−0.038 (.764)	0.008 (.947)	0.109 (.385)					
pdDMN	−0.112 (.369)	−0.166 (.183)	0.149 (.234)	−0.236 (.056)*				
Vis	−0.118 (.345)	−0.034 (.786)	0.057 (.652)	−0.198 (.110)	−0.250 (.043)*			
Aud	−0.190 (.127)	−0.166 (.182)	−0.077 (.538)	−0.182 (.144)	0.011 (.931)	0.143 (.251)		
Sens	−0.045 (.722)	−0.170 (.172)	−0.077 (.537)	−0.074 (.554)	0.067 (.591)	0.043 (.733)	−0.046 (.716)	

Abbreviations: ADAS Cog, (Mod), modified version of the Alzheimer's Disease Assessment Scale-cognitive subscale; Aud, auditory network; iFC, intrinsic functional connectivity; lAtt, left attention network; pdDMN, posterior-dorsal default mode network; pvDMN, posterior-ventral default mode network; rAtt, right attention network; Sens, sensorimotor network; Vis, visual network.

NOTE. No partial Pearson correlation coefficients (r), controlling for age and sex, were significant following correction for multiple comparisons (corrected $a \leq .006$).

*Significant/marginally significant correlations at $P \leq .05$, before multiple comparison correction.

characterized as a disorder in which multiple iBNs, alongside the DMN, are affected [8,9,14–17,42]. Our results suggest that a global decrement in iFC within a broad range of iBNs can be observed with increased cognitive impairment in Aβ-positive subjects. Recent findings [43] may offer some insight into this global iFC decrement in AD. Having been interested in the relationship between neuronal and hemodynamic activity, Matsui et al. found that the neuronal coactivations that represent iBNs are embedded in a frequent global sweep of activity across the entire cortex, neuronal coactivations that are followed by similar coactivations in hemodynamic signaling. Such findings suggest a reliance of the intrinsic functional connections that define iBNs on the initial global wave of neuronal activity and so an impairment in the global wave may lead to an impairment in the delicate timing of the neuronal and hence the hemodynamic coactivations (iFC) that occur within iBNs. This impairment, if indeed the case, would be expected to occur within iBNs across the entire cortex, rather than being localized to any one network. Calcium signaling has been found to be disrupted in mice models of AD [44], and hence our findings and those of Matsui et al. may offer insight into how an impairment in neuronal signaling may be related to iFC impairments and subsequently cognitive impairment in AD.

4.3. Limitations

The aim of our study was to identify changes in iFC within and between a wide range of iBNs across the entire spectrum of AD. Having used a cross-sectional sample of Aβ-positive subjects to define the spectrum, a further study with a longitudinal design may better define the progression of iFC changes. One should also consider the role that other aspects of AD pathophysiology, such as Aβ deposition, tau pathology, and vascular changes, may play in the progression of iFC alterations and cognitive impairment across the AD spectrum. Furthermore, although used as a standard measure to assess cognitive impairment in AD, the ADAS (Cog) scale has been criticized for lack of validity at various stages of AD. The scale has been found to be accurate for patients with moderate AD, whereas patients with MCI and mild AD have been reported to display ceiling effects. Similarly, patients in advanced AD stages with impaired language abilities have shown floor effects with this measure [45]. Thus, the ADAS (Cog) scale may not have been able to adequately define the progression of cognitive impairment in our sample. Finally, our regression of the whole-brain signal during rsfMRI data preprocessing may have induced artificial correlations in our data [46].

5. Conclusion

With increased cognitive impairment along the AD spectrum, decrements in iFC within a wide range of iBNs can be seen, leading to a characterization of AD as a disorder of multiple networks.

Supplementary data

Supplementary data related to this article can be found at http://dx.doi.org/10.1016/j.dadm.2016.11.006.

RESEARCH IN CONTEXT

1. Systematic review: Using standard literature sources (e.g., PubMed), current knowledge concerning the link between intrinsic functional connectivity changes and cognitive impairment across the Alzheimer's disease (AD) spectrum was identified. Although there was extensive research concerning the default mode network, research investigating a broad range of other intrinsic brain networks (iBNs) in AD was relatively infrequent.
2. Interpretation: Our results expand on previous findings concerning the role of various iBNs in AD, showing that AD can be characterized as a disorder of intrinsic functional connectivity impairment within multiple iBNs alongside the default mode network, impairments that are strongly correlated with cognitive impairment across the whole AD spectrum.
3. Future directions: The mechanisms underlying a global iBN impairment and their links to AD pathophysiology require clarification.

References

[1] Alzheimer's Disease International. The global impact of dementia. An analysis of prevalence, incidence, cost and trends. 2015. Available at: https://www.alz.co.uk/research/WorldAlzheimerReport2015.pdf. Accessed May 12, 2016.
[2] Braak H, Braak E. Neuropathological stageing of Alzheimer-related changes. Acta Neuropathol 1991;82:239–59.
[3] Nelson PT, Braak H, Markesbery WR. Neuropathology and cognitive impairment in Alzheimer disease: a complex but coherent relationship. J Neuropathol Exp Neurol 2009;68:1–14.
[4] Busche MA, Eichhoff G, Adelsberger H, Abramowski D, Wiederhold KH, Haass C, et al. Clusters of hyperactive neurons near amyloid plaques in a mouse model of Alzheimer's disease. Science 2008;321:1686–9.
[5] Busche MA, Kekuš M, Adelsberger H, Noda T, Förstl H, Nelken I, et al. Rescue of long-range circuit dysfunction in Alzheimer's disease models. Nat Neurosci 2015;18:1623–30.
[6] Sperling RA, LaViolette PS, O'Keefe K, O'Brien J, Rentz DM, Pihlajamaki M, et al. Amyloid deposition is associated with impaired default network function in older persons without dementia. Neuron 2009;63:178–88.

[7] Drzezga A, Becker JA, Van Dijk KR, Sreenivasan A, Talukdar T, Sullivan C, et al. Neuronal dysfunction and disconnection of cortical hubs in non-demented subjects with elevated amyloid burden. Brain 2011;134:1635–46.
[8] Myers N, Pasquini L, Göttler J, Grimmer T, Koch K, Ortner M, et al. Within-patient correspondence of amyloid-β and intrinsic network connectivity in Alzheimer's disease. Brain 2014;137:2052–64.
[9] Grothe MJ, Teipel SJ. Spatial patterns of atrophy, hypometabolism, and amyloid deposition in Alzheimer's disease correspond to dissociable functional brain networks. Hum Brain Mapp 2015;37:35–53.
[10] Elman JA, Madison CM, Baker SL, Vogel JW, Marks SM, Crowley S, et al. Effects of beta-amyloid on resting state functional connectivity within and between networks reflect known patterns of regional vulnerability. Cereb Cortex 2016;26:695–707.
[11] Damoiseaux JS, Rombouts SA, Barkhof F, Scheltens P, Stam CJ, Smith SM, et al. Consistent resting-state networks across healthy subjects. Proc Natl Acad Sci U S A 2006;103:13848–53.
[12] Allen EA, Erhardt EB, Damaraju E, Gruner W, Segall JM, Silva RF, et al. A baseline for the multivariate comparison of resting-state networks. Front Syst Neurosci 2011;5:2.
[13] Raichle ME. The brain's default mode network. Annu Rev Neurosci 2015;38:433–47.
[14] Wang K, Liang M, Wang L, Tian L, Zhang X, Li K, et al. Altered functional connectivity in early Alzheimer's disease: a resting-state fMRI study. Hum Brain Mapp 2007;28:967–78.
[15] Agosta F, Pievani M, Geroldi C, Copetti M, Frisoni GB, Filippi M. Resting state fMRI in Alzheimer's disease: beyond the default mode network. Neurobiol Aging 2012;33:1564–78.
[16] Brier MR, Thomas JB, Snyder AZ, Benzinger TL, Zhang D, Raichle ME, et al. Loss of intranetwork and internetwork resting state functional connections with Alzheimer's disease progression. J Neurosci 2012;32:8890–9.
[17] Lim HK, Nebes R, Snitz B, Cohen A, Mathis C, Price J, et al. Regional amyloid burden and intrinsic connectivity networks in cognitively normal elderly subjects. Brain 2014;137:3327–38.
[18] Jones DT, Knopman DS, Gunter JL, Graff-Radford J, Vemuri P, Boeve BF, et al. Cascading network failure across the Alzheimer's disease spectrum. Brain 2016;139:547–62.
[19] Price JL, Morris JC. Tangles and plaques in nondemented aging and "preclinica" Alzheimer's disease. Ann Neurol 1999;45:358–68.
[20] Aisen PS, Petersen RC, Donohue MC, Gamst A, Raman R, Thomas RG, et al. Clinical core of the Alzheimer's Disease Neuroimaging Initiative: progress and plans. Alzheimers Dement 2010;6:239–46.
[21] Wechsler D, Stone CP. Wechsler memory scale-revised. New York: Psychological Corporation; 1987.
[22] McKhann G, Drachman D, Folstein M, Katzman R, Price D, Stadlan EM. Clinical diagnosis of Alzheimer's disease: Report of the NINCDS-ADRDA Work Group* under the auspices of Department of Health and Human Services Task Force on Alzheimer's Disease. Neurology 1984;34:939–44.
[23] Fleisher AS, Chen K, Liu X, Roontiva A, Thiyyagura P, Ayutyanont N, et al. Using positron emission tomography and florbetapir F 18 to image cortical amyloid in patients with mild cognitive impairment or dementia due to Alzheimer disease. Arch Neurol 2011;68:1404–11.
[24] Rosen WG, Mohs RC, Davis KL. A new rating scale for Alzheimer's disease. Am J Psychiatry 1984;141:1356–64.
[25] Robert P, Ferris S, Gauthier S, Ihl R, Winblad B, Tennigkeit F. Review of Alzheimer's disease scales: is there a need for a new multi-domain scale for therapy evaluation in medical practice? Alzheimers Res Ther 2010;2:1.
[26] Graham DP, Cully JA, Snow AL, Massman P, Doody R. The Alzheimer's Disease Assessment Scale-Cognitive subscale: normative data for older adult controls. Alzheimer Dis Assoc Disord 2004; 18:236–40.
[27] Stern RG, Mohs RC, Davidson M, Schmeidler J, Silverman J, Kramer-Ginsberg E, et al. A longitudinal study of Alzheimer's disease: measurement, rate, and predictors of cognitive deterioration. Am J Psychiatry 1994;151:390–6.
[28] Weyer G, Erzigkeit H, Kanowski S, Ihl R, Hadler D. Alzheimer's Disease Assessment Scale: reliability and validity in a multicenter clinical trial. Int Psychogeriatr 1997;9:123–38.
[29] Mohs RC, Knopman D, Petersen RC, Ferris SH, Ernesto C, Grundman M, et al. Development of cognitive instruments for use in clinical trials of antidementia drugs: additions to the Alzheimer's Disease Assessment Scale that broaden its scope. Alzheimer Dis Assoc Disord 1997;11:13–21.
[30] Skinner J, Carvalho JO, Potter GG, Thames A, Zelinski E, Crane PK, et al. The Alzheimer's disease assessment scale-cognitive-plus (ADAS-Cog-Plus): an expansion of the ADAS-Cog to improve responsiveness in MCI. Brain Imaging Behav 2012;6:489–501.
[31] Chao-Gan Y, Yu-Feng Z. DPARSF: a MATLAB toolbox for "pipeline" data analysis of resting-state fMRI. Front Syst Neurosci 2010;4:13.
[32] Tanabe J, Miller D, Tregellas J, Freedman R, Meyer FG. Comparison of detrending methods for optimal fMRI preprocessing. Neuroimage 2002;15:902–7.
[33] Power JD, Barnes KA, Snyder AZ, Schlaggar BL, Petersen SE. Spurious but systematic correlations in functional connectivity MRI networks arise from subject motion. Neuroimage 2012;59:2142–54.
[34] Satterthwaite TD, Elliott MA, Gerraty RT, Ruparel K, Loughead J, Calkins ME, et al. An improved framework for confound regression and filtering for control of motion artifact in the preprocessing of resting-state functional connectivity data. Neuroimage 2013; 64:240–56.
[35] Calhoun VD, Adali T, Pearlson GD, Pekar JJ. A method for making group inferences from functional MRI data using independent component analysis. Hum Brain Mapp 2001;14:140–51.
[36] Beckmann CF, Smith SM. Probabilistic independent component analysis for functional magnetic resonance imaging. IEEE Trans Med Imaging 2004;23:137–52.
[37] Himberg J, Hyvärinen A. Icasso. software for investigating the reliability of ICA estimates by clustering and visualization. In Proc. 2003 IEEE Workshop on Neural Networks for Signal Processing (NNSP2003):259–68.
[38] IBM Corp. IBM SPSS statistics for Windows, Version 22.0. Armonk, NY: IBM Corp; 2013.
[39] Song XW, Long X, Zang Y. RESTing-state fMRI data analysis toolkit (REST) manual. Beijing: Beijing Normal University; 2008.
[40] Deco G, Corbetta M. The dynamical balance of the brain at rest. Neuroscientist 2011;17:107–23.
[41] Greicius MD, Srivastava G, Reiss AL, Menon V. Default-mode network activity distinguishes Alzheimer's disease from healthy aging: evidence from functional MRI. Proc Natl Acad Sci U S A 2004; 101:4637–42.
[42] Koch K, Myers NE, Göttler J, Pasquini L, Grimmer T, Förster S, et al. Disrupted intrinsic networks link amyloid-β pathology and impaired cognition in prodromal Alzheimer's disease. Cereb Cortex 2015; 25:4678–88.
[43] Matsui T, Murakami T, Ohki K. Transient neuronal coactivations embedded in globally propagating waves underlie resting-state functional connectivity. Proc Natl Acad Sci U S A 2016; 113:6556–61.
[44] Demuro A, Parker I, Stutzmann GE. Calcium signalling and amyloid toxicity in Alzheimer disease. J Biol Chem 2010;285:12463–8.
[45] Doraiswamy PM, Kaiser L, Bieber F, Garman RL. The Alzheimer's Disease Assessment Scale: evaluation of psychometric properties and patterns of cognitive decline in multicenter clinical trials of mild to moderate Alzheimer's disease. Alzheimer Dis Assoc Disord 2001; 15:174–83.
[46] Murphy K, Birn RM, Handwerker DA, Jones TB, Bandettini PA. The impact of global signal regression on resting state correlations: are anti-correlated networks introduced? Neuroimage 2009; 44:893–905.